Amphiphilic properties of dodecylammonium chloride/sodium 4-(1-pentylheptyl) benzenesulfonate aqueous mixtures and study of the catanionic complex

Tea Mihelj*, Vlasta Tomašić

Department of Physical Chemistry, Ruđer Bošković Institute, POB 180, Zagreb, HR–10002 Croatia

* Corresponding author:
Tea Mihelj
Ruđer Bošković Institute
Bijenička c. 54, P.O.Box 180
HR-10002 Zagreb, Croatia
Tel.: +385-1-4571-211
Fax: +385-1-4680-245
E-mail address: Tea.Mihelj@irb.hr

Abstract

Surfactants are often used in supramolecular chemistry, due to their ability to self-organize. Surfactant molecules aggregate spontaneously and reversibly to adopt a defined intermolecular arrangement. In this work, general phase behavior, adsorption and association in aqueous mixtures of dodecylammonium chloride, DACl and sodium 4-(1-pentylheptyl) benzenesulfonate, NaDBS, were studied by a combination of techniques including surface tension and conductivity measurements, light scattering and optical microscopy. The strong synergistic properties of the system were brought out with the Regular Solution Theory. Various colloidal objects are observed in wide range of composition: conventional small vesicles, large giant multilamellar or multivesicular vesicles. An excess of NaDBS provides extremely large tubular and elongated multilamellar vesicles. The new catanionic 1:1 complex, dodecylammonium-4-(1-pentylheptyl) benzenesulfonate, formed in the equimolar conditions is a result of intramolecular charge neutralization. The thermal properties of this solid compound were examined by thermal polarizing microscopy, differential scanning calorimetry, and X-ray diffraction. The most probable ion-pair amphiphilic cluster of crystal smectic phase, at room temperature, consists of ionic groups formed in ordered layers with dodecyl chains packed into somewhat disordered layers, tilted to the layer plane.

Key words: surfactant mixtures, catanionic surfactant, mesomorphism, wide angle X-ray scattering, dodecylammonium-4-(1-pentylheptyl) benzenesulfonate

Introduction

Surfactant molecules are organic amphiphilic compounds that possess the property of adsorbing onto the surfaces and interfaces, as well as the ability to spontaneously self-organize into the structures of a defined intermolecular arrangement. Two oppositely charged surfactants have a strong tendency to mix and form a range of structures governed by electrostatic interactions, geometrical packing, repulsive hydration forces and attractive hydrophobic interactions [1–4]. Common examples include formation of micelles, vesicles, bilayer lamellae, and liquid crystal phases. Mixed cationic-anionic surfactant systems have been intensively studied during a long period of time, mainly in relatively dilute systems, with careful distinction between different segregative and associative phase separation phenomena [5, 6]. The phase behavior of such systems should provide an appropriate starting point for analysis of rather complex patterns.

Alkylbenzenesulfonates (ABS) have been the major components of laundry detergents and cleaners. Due to the biodegradation problems, the ABS with branched alkyl chains have been replaced by linear alkylbenzene sulfonates (LAS) [7, 8]. However, LAS is not a pure compound but a mixture of isomers, for example, the commercial linear *p*-dodecylbenzenesulfonates is a mixture of homologues with benzene ring attached at different carbon atom along with the alkylchain (abbreviated C1–C6) [9]. The physico-chemical properties of the isomers thus depend on the position of the headgroup because it affects significantly the local molecular packing constraints [9]. In general with the headgroup moves from the end to the center of the dodecyl chain, the hydrophobicity, Krafft temperature, as well as surface tension monotonically decrease [10], but the critical aggregation concentrations and the minimum area per molecule increase [9]. Approximately linear relationships exist between headgroup position along dodecyl chain and log critical aggregation or micellization concentrations, minimum area per molecule at the air-aqueous solution interface, standard free energy of micellization, and maximum surface excess [9, 11, 12]. Obviously in the mixture with cationic surfactants, the exact molecular structure of LAS strongly influences not only the effective molecular shape or ability to self-assemble into aggregate, but also the aggregate packing constraints in catanionic complexes. Recent serial study [3, 4] revealed that interactions of oppositely charged surfactant species under equimolar conditions lead to formation of stable, usually crystalline molecular complexes, especially in the systems with quaternary ammonium salts. Such complexes behave as novel, catanionic surfactants, with their own *cmc*'s, inherent Krafft points, solubilization and

crystallization [4, 13]. Thermodynamic parameters and phase transition temperatures change linearly with the total number of carbon atoms in a straight hydrocarbon chain. The same chain lengths of both tails in the catanionic bilayer allow denser and more ordered molecular packing [3, 14, 15]. A common feature for most catanionics is lamellar structure of solid crystal phases and smectic S_A phase as a liquid crystal phase. In general, the structure can be fine-tuned by tailoring the nature of the components, owing to the interplay between electrostatic effects, surfactant molecular size and geometry [16], and hydrogen bonding network.

This work presents physicochemical and microstructural study of the sodium-4-(1-pentylheptyl) benzenesulfonate, NaDBS/ dodecylammonium chloride, DACl, aqueous mixed system, including synergistic properties and the formation conditions of the new catanionic compound, dodecylammonium-4-(1-pentylheptyl) benzenesulfonate, DA-DBS, which are not previously reported, probably due to the NaDBS purity problems. The solid catanionics with benzenesulfonate anions were not previously reported, mostly because of questions about NaDBS purity. The study on the aqueous surfactant mixtures may assist in understanding the principles governing aggregate formation, and the analysis of the catanionic structure should provide more information on the nature of self-organized processes between cationic and anionic surfactants.

Experimental

Materials

Dodecylammonium chloride, DACl, was prepared and purified as described earlier [4], which has low Krafft temperature (289 K) as well known [17, 18]. Sodium 4-(1-pentylheptyl) benzenesulfonate, NaDBS, was a present (analytically pure) from courtesy of the Henkel Co., Germany, which was further purified by multiple recrystallization from ethanol-water to remove excess of inorganic electrolyte. Its purity has been checked by IR, high performance liquid chromatography– electrospray tandem mass spectrometry (HPLC-ESI-MS/MS) characterization and surface tension measurements. The IR spectrum showed only the strong band at 855 cm^{-1}, typical of the *para* disubstituted benzene isomer, and no minima were observed in the surface tension versus concentration plots. HPLC-grade acetonitrile (≥ 99.93 %) and 4-octylbenzenesulfonic acid and triethylamine were purchased

from Sigma Aldrich. Acetic acid (100 %) was purchased from AppliChem GmbH, Denmark. The commercial C_{10}-C_{13} alkylammonium benzenesulfonate mixture of homologues and isomers for the preparation of standard solutions were obtained from Masso and Carol (Spain). Liquid chromatography-UV–electrospray-ion-trap mass spectrometry system (110 Series LC/MSD Agilent Technologies, Germany) is equipped with an automatic injector. The stationary phase was Nova Pack C_{18} 4 μm column (300 mm x 3.9 mm, Waters P/N WATO11695) and the mobile phase used for chromatographic separations was a mixture of solvent 1 (acetonitrile : water = 70 : 30) and solvent 2 (water), both containing 2.5 mM acetic acid and 2.5 mM triethylamine. MS analysis was carried out in the ESI (-) mode, with the excitation of the ions through collision with helium. Quantitation was carried out under full scan conditions in the *m*/*z* range 150-360, using the extracted ion chromatograms at the *m*/*z* of the selected fragments for each isomer (C_2 184, C_3 198, C_4 212, C_5 226, and C_6 240) and measuring the corresponding peak areas. The purity of NaDBS was established to be ≈ 98 wt % (Table 1) and the homologue distribution was found as follows, in w_t %: undecyl, 1.20; dodecyl, 98.41; tridecyl, 0.39 (Fig. 1).

The phase diagram of NaDBS shows isotropic phase only within limited surfactant concentration and temperature ranges [7, 18–20]. Therefore, all experiments were carried out at 303 K in order to approach experimental conditions above the Krafft temperature of both reactants. Water used in all experiments was purified using a Millipore MilliQ Plus Ultrapure Water System (Millipore, Australia).

Fig.1

Table 1

Preparation of aqueous surfactant mixtures and solid surfactant molecular complex

Aqueous surfactant mixtures were prepared either with constant DACl and increasing NaDBS concentration or *vice versa*, using the sequence of addition: aqueous solution of anionic surfactant first, and then of cationic surfactant. Solutions were gently mixed for 5 minutes after preparation, and allowed to equilibrate undisturbedly for one day in a thermostated bath at 303 K before measurements. The detailed preparation has been described earlier [3, 4, 13–16]. The examination was performed in order to simulate and screen the conditions and behavior in native systems, as a part of more complex natural environment.

Although inorganic electrolyte (NaCl) is not actively added in examined system, its concentration increases slightly and continuously parallel with the concentrations of interacting surfactant species and the inevitable formation of dissociate counterions takes place. Also, the fixed aging time is always respected, irrespective to equilibration rates of different processes involved.

Solid complex DA-DBS was prepared by mixing equimolar ($7 \cdot 10^{-2}$ mol dm^{-3}, point **D** in precipitation diagram, Fig. 2) aqueous solutions of anionic and cationic surfactants intensively for 45 minutes at approximately 343 K and the mixture was left aging undisturbedly for one week at room temperature. The precipitated catanionic surfactant was filtered through Millipore filter type HA with 0.45 μm pore size, washed with cold water and diethyl ether, in order to remove coprecipitated salt and possibly coprecipitated anionic or cationic surfactant, and dried under reduced pressure at room temperature till constant mass was obtained (32 hours). Such powdered light yellow mass was stored in a dessicator, protected from light and moisture before further analysis.

Measurements

Conductivity measurements were performed with a Mettler MPC 227 Conductivity Meter (Columbus, OH) and surface tension measurements with a circulating autothermostated Interfacial Tensiometer K100, Krüss (Hamburg, Germany). Microstructures and visible change of the turbidity in the solution were examined using a combination of light microscopy and dynamic light-scattering, DLS (Zetasizer Nano ZS, Malvern Instruments, Worcestershire, UK) equipped with a 532 nm "green" laser. Detection occurred at 173^{o} angle in glass cuvettes. A latex standard of uniform particle size of 20 nm was used to evaluate the accuracy of the measurements. Mean hydrodynamic diameter of vesicles, d_h, is estimated using Debye-Einstein-Stokes equation, data are reported as number distribution, and represented as a mean value of at least six measurements.

The purity of catanionic compound (1:1 adduct, $C_{30}H_{57}NO_3S$, Mw = 511.85) was identification by elemental analysis (Perkin-Elmer Analyzer PE 2400 Series 2), which gives(mass percentages): C, 70.41; H, 11.23; N, 2.77 %, in very good agreement with calculation: C, 70.40; H, 11.22; N, 2.74 %.

Thermogravimetric analysis, TGA, was performed from room temperature to 560 K, with a Mettler TA 4000 System, and a decomposition temperature T_d/ K = 530, was obtained. Thermal properties were examined by differential scanning calorimetry, DSC, using Perkin Elmer Pyris Diamond DSC calorimeter in N_2 atmosphere, equipped with a model Perkin Elmer 2P intra-cooler. Sample was heated from room temperature to 400 K and cooled back to RT at a rate of 5 K min^{-1}. The transition enthalpy, ΔH/ kJ mol^{-1}, was determined from the peak area of the DSC thermogram; and the corresponding entropy change, ΔS/ J mol^{-1} K^{-1}, was calculated using the maximal transition temperature. All results are mean values of several independent, first run measurements, due to different periods of catanionic surfactant recovery to original state after heating [3, 4, 14, 15].

Detection and microstructural identification of different phases and optical textures in surfactant mixtures and of solid sample were carried out with a Leica DMLS polarized optical light microscope, equipped with a Sony digital camera (SSC-DC58AP), and a Linkam LNP (THMS 600) hot stage with liquid nitrogen cooling.

Wide angle X-ray scattering (WAXS) measurements were performed by an automatic X-ray powder diffractometer, Philips PW 3710, with monochromatized Cu Kα radiation (λ/ Å = 1.54056) and proportional counter. Patterns were recorded at room temperature, RT. The overall diffraction angle region was 2θ/ ^{o} = 3–50. The interlayer spacing, d_{hkl}, was calculated according to Bragg's law.

Interpretation of data

The precipitation boundaries as well as macroscopic boundaries of phase separation for the DACl-NaDBS/H_2O system (Fig. 2) were examined in a wide concentration range of each component, taking as maximum concentration of the reactant not resulting in significant changes of turbidity or solid phase occurrence. The critical micelle concentration, *cmc*, of single surfactant DACl and NaDBS, as well as that of mixtures, is given by the intersection of the two linear sections of surface tension, γ, or conductivity, κ, versus logarithm concentration curves by the method of linear regression with fitting correlation coefficients equal or better than 0.99. The apparent degree of counterion dissociation from the micelle/solution interface, α, is the ratio of the slopes, B_1 and B_2, of the κ *vs.* concentration lines above and below the

cmc respectively [19]: $\alpha = \frac{B_2}{B_1}$ (1).

The composition of the mixed monolayer at the solution/air interface, the surface activity coefficients f and the mixed monolayer interaction parameter β_{mon}, were calculated using Regular Solution Theory [20] based on surface tension measurements:

$$\frac{X_{DACl}^2 \ln(\alpha_{DACl} c_{DACl+NaDBS}/c_{DACl} X_{DACl})}{(1-X_{DACl})^2 \ln[(1-\alpha_{DACl}) c_{DACl+NaDBS}/(1-X_{DACl}) c_{NaDBS}]} = 1 \quad (2),$$

where c_{DACl} and c_{NaDBS} are the concentrations of individual DACl and NaDBS solutions and and $c_{DACl+NaDBS}$ the concentration of their mixture solution, required to give a same surface tension reduction; X_{DACl} is the mole fraction of individual surfactant DACl in the mixed monolayer, and α_{DACl} its molar fraction in the solution. The surface molecular interaction parameter, β_{mon}, in the mixed monolayer and the surface activity coefficients, f_{DACl} and f_{NaDBS} for individual surfactants were calculated as follows (3) - (5):

$$\beta_{mon} = \frac{\ln(\alpha_{DACl} c_{DACl+NaDBS}/c_{DACl} X_{DACl})}{(1-X_{DACl})^2} \quad (3),$$

$$f_{DACl} = \exp[\beta_{mon}(1 - X_{DACl})^2] \quad (4),$$

$$f_{NaDBS} = \exp[\beta_{mon}(X_{DACl})^2] \quad (5).$$

The same equations (2) – (5) were used to calculate the parameters for mixed micelles using the *cmc*'s of individual surfactants and of their mixture at molar fraction α instead of c_{DACl}, c_{NaDBS}, and $c_{(DACl+NaDBS)}$.

The maximum surface excess, Γ_{max}/mol m^{-2} at the air/solution interface was calculated from the maximum slope of the linear part of the γ *vs*. logc_{DACl} or logc_{NaDBS} curve, for the surfactant concentrations lower than *cmc* and at constant temperature, by applying the Gibbs adsorption isotherm [21]: $\Gamma_{max} = -\frac{1}{2.303\, n\, R\, T} \left(\frac{\partial \gamma}{\partial \log c}\right)_T$ (6),

where n represents the number of species at the interface, whose concentration changes with surfactant concentration, R/J K^{-1} mol^{-1} = 8.314 is the gas constant, T/K is the thermodynamic temperature, $(\partial\gamma/\partial \log c)_T$ is the slope of the surface tension *vs*. log$c$ curve and c is the surfactant concentration (c_{DACl} or c_{NaDBS}).

The minimum area occupied by a surfactant molecule at the air/solution interface, A_{min}/nm^2, where N_A is Avogadro's number, can be calculated from the relation [21]:

$$A_{min} = \frac{10^{18}}{\Gamma_{max} N_A} \quad (7).$$

The shape of self-assembled structures in the solution can be predicted with the critical packing parameter P or the shape factor [22]: $P = \frac{V}{A_{\min} l}$ (8).

Critical packing parameter was calculated where the following molecule dimensions are taken: DACl, l_1 = 1.668 nm, V_1 = 0.3502 nm^3 [21] and NaDBS, V_2 = 0.3351 nm^3.

The standard free energy of adsorption, at the air/solution interface ΔG^{o}_{ads} [23], has been evaluated by the equation (9): $\Delta G^{o}_{ads} = \Delta G^{o}_{mic} - (\frac{\pi_{cmc}}{\Gamma_{max}})$ (9),

where ΔG^{o}_{mic} is the standard free energy of micellization per mole of alkyl chain (10):

$\Delta G^{o}_{mic} = (1 + \beta)\, RT \ln cmc$ (10),

where β is the degree of counterion association to the micelle solution/interface ($\beta = 1 - \alpha$), and π_{cmc} is the surface pressure at the *cmc*: $\pi_{cmc} = \gamma_{H_2O} - \gamma_{cmc}$ (11),

where γ_{H_2O} is surface tension of water and γ_{cmc} is the surface tension of the surfactant solution at the *cmc*.

Results and discussion

The partial phase diagram of pure NaDBS in water was previously studied [9, 24]. A multitude of phases [7,19] were observed in wide temperature and concentration ranges. Examination of the isotropic region showed the existence of spherical micelles (cmc_{NaDBS}/mmol dm^{-3} = 2.70–3.12) [18–20], transformation to oblate micelles at $7.78 \cdot 10^{-3}$ mol dm^{-3} [24, 25], and transition to vesicular dispersion at $8.30 \cdot 10^{-2}$ mol dm^{-3} at 303 K [24]. At this temperature, electrolyte addition to pure NaDBS (c_{NaDBS}/mmol dm^{-3} = 2.86) induces transition of isotropic micellar to an anisotropic lamellar solution at $c_{NaCl} > 6.67 \cdot 10^{-2}$ mol dm^{-3}, and slightly increases the very low Krafft temperature in systems with c_{NaCl} = 1 mol dm^{-3} [7]. Having in mind these conditions and to restrict our examinations to the sole isotropic phase of NaDBS (monomers and micelles only), our experiments have been carried out at fixed temperature (303 K), at $c_{NaDBS} < 8.00 \cdot 10^{-2}$ mol dm^{-3}. In the DACl-NaDBS-H_2O system, the maximum concentration of NaCl formed (c_{NaCl} = $7.00 \cdot 10^{-2}$ mol dm^{-3}) is reached only in peripheral precipitation diagram region where electrostatic interaction between stoichiometric

composition of cationic and anionic surfactant and precipitation of insoluble catanionic surfactant overcome vesiculation forces.

General phase behavior of the DACl – NaDBS – water system

The partial precipitation diagram of the DACl-NaDBS aqueous mixture in a dilute water rich corner is shown in Fig. 2. The diagram is result of combined data from visual observation of turbidity and precipitation, data from light microscopy, tensiometry, conductometry, light scattering and electrophoresis. Determined *cmc*s of components are $cmc_{\mathrm{DACl}} = 1.48 \cdot 10^{-2}$ mol dm^{-3} and $cmc_{\mathrm{NaDBS}} = 3.10 \cdot 10^{-3}$ mol dm^{-3}. The value of cmc_{NaDBS} is very similar to that previously determined [25, 26], although the transition to oblate micelles is not detected. The system is examined at constant temperature within wide concentration ranges of components, from very dilute to approximately four to six times *cmc* of DACl or NaDBS, and mainly after 24 h of aging. The dash-dot line denotes stoichiometric bulk composition, dividing the picture into NaDBS and DACl rich areas. Three clear regions are delimited, I is the premicellar region, and II and III are recognized as mixed micelles regions. The values of the corresponding *cmc* of surfactant in excess with small addition of oppositely charged surfactant are denoted with short dotted lines. Spontaneous formation of vesicles was obtained in the turbid region IV, where flat lamellae, lamellae bending into tubules, long tubular vesicles, or embedded vesicles of various shapes, sizes and level of encapsulation were also found. This is area were parts of partial precipitation, and vesicles - precipitate coexistence region exist. Intensive precipitation of insoluble catanionic DA-DBS occurs in the region V at higher concentration of components and strictly around the stoichiometric bulk composition. Concentration points **A** and **B** in the area IV were additionally examined by optical microscopy. Size of vesicles prepared in the equimolar area IV of precipitation diagram (Fig. 2) noted with **C** ($c_{\mathrm{DACl}} = c_{\mathrm{NaDBS}} = 1.00 \cdot 10^{-4}$ mol dm^{-3}) was observed by means of a DLS technique, and **D** represents the equivalent concentration ($c_{\mathrm{DACl}} = c_{\mathrm{NaDBS}} = 7.00 \cdot 10^{-2}$ mol dm^{-3}) at which the solid catanionic compound is precipitated and isolated. Fig. 3 shows representative micrographs of samples prepared at the stoichiometric bulk composition, and Fig. 4 with one of the surfactant in excess, taken 24 hours after preparation.

Fig. 2

Fig. 3

Fig. 4

Small and closed vesicles appear spontaneously in DACl-NaDBS mixture aqueous solution one hour after preparation and along equimolar ratio of the components and concentration above $2 \cdot 10^{-5}$ mol dm^{-3}. In more concentrated conditions, vesicles become deformed, with irregular shapes and variable habitus (Fig. 3a), and polydispersed (Fig. 3b and c), until the concentration of $2 \cdot 10^{-3}$ mol dm^{-3}, where preferred precipitation coexist with small vesicles (Fig. 3d). Apart from polydisperse and closely packed vesicles, giant multilamellar (Fig. 3b) and multivesicular (Fig. 3c) vesicles are formed at higher equivalent surfactant concentrations. In one word, the quantity and diameter of closed vesicles grow, and quality changes with the increase of total equimolar surfactant concentrations. Simultaneously, the spontaneous growth of inorganic electrolyte concentration (present counterions) occurs. The vesicle systems are so specific that they can be directly observed under light microscope due to their huge diameter, without chemical fixation, staining, replication, or utilizing a fast-frozen hydrated sample in a transmission electron microscope

The vesicles with neutralized charge (Fig. 3) differ in properties from those formed in the excess of one component (Fig. 4). Excess of DACl induces formation of small and larger spherical and, to some extent open cylindrical vesicles (Figs. 4a and b). Excess of NaDBS provides, besides formation of spherical vesicles, the formation of extremely large tubular and elongated multilamellar vesicles (Figs. 4c and d). Moreover, the values of critical packing parameters (Table 2) for systems formed in excess of NaDBS are, to some extent, higher than of those prepared in excess of DACl, suggesting preferable formation of more planar than closed bilayers. The tubules are longer than 100 μm approaching macroscopic dimensions (Figs. 4c and d), and with multilamellar walls about 17 μm thick (Fig. 4d). Interconversion of spherical into tubular aggregates is a consequence of changed conditions (primarily owing to total surfactant concentration and related electrolyte variations). In order to change the effective spontaneous curvature of the mixed bilayer in terms of extended bilayer, and to deform it into tubular vesicles shape, the membrane elastic resistance forces must be balanced by the ones generated with the addition of NaDBS in excess. To conclude, this transformation seems to be the consequence of the coexistence between charged species in excess and those of neutralized charge, which leads to new balance of the intrabilayer forces in order to reduce the free energy increase.

Table 2

Taking into account the approximate effective ionic radii of ammonium and sulfonate groups in comparison with the thickness and branching of hydrocarbon chains, the geometric structure of DACl and NaDBS are cone and truncated cone respectively [9, 27]. It seems that the steric repulsion between the double tails of NaDBS and the hydrophobic chain of DACl makes it difficult to stack together tightly. As shown in Table 2, the calculated value of critical packing parameter for equimolar mixture of DACl and NaDBS is 0.73. According to literature data [22] for $P = ½ – 1$, as a result of intra-molecular charge neutralization and steric repulsion between tails, the catanionic complex forms truncated cone approaching the shape of cylinder, *i.e.* cuplike structure (Scheme 1), favorable for vesicle formation.

Scheme 1

Unlike previously described regions, only small, uniform, monodisperse and spherical vesicles are formed for shorter aging time in the equimolar area and in lower concentration region, below the *cmc* of individual components. Such vesicles were appropriate for measurements of their hydrodynamic radii, d_h/nm. System prepared in the equimolar area of the precipitation diagram, noted **C**, where $c_{NaDBS} = c_{DACl} = 1 \cdot 10^{-4}$ mol dm^{-3}, was observed within one week. The *cmc* of this mixture amounts to $3.25 \cdot 10^{-6}$ mol dm^{-3} and mixed micelle to unilamellar or oligolamellar vesicle transition occurs parallel with the concentration increment along the equimolar line. Small monodispersed vesicles (Fig. 5) with $d_h \approx 100$ nm appear 2 min after preparation and grow into bigger aggregates (750 nm) after 100 min of aging. The second fraction with larger hydrodynamic radius appears after 4500 min of aging and follows its individual growth from d_h/nm = 1000–2000, resulting in bimodal distribution. The vesicles remain stable for at least two weeks, and correspond to small, medium and large/gigantic ones. The growth is the result of their spontaneous aggregation in the slow relaxation process during which small metastable vesicles lower their high energy of bending when transforming into large ones. This may occur by fusion which includes overlapping of two vesicle bilayers into one and merging of contents, or with ripening of vesicular dispersions [28]. In contrast to small [29] and stable ones, observed for similar catanionic mixture, vesicles studied in this work have much greater size and their polydispersity increases dramatically with the increase of surfactant concentration and aging.

Fig. 5

Adsorption and association in DACl – NaDBS – water mixtures

The study of adsorption and association in DACl – NaDBS – water mixtures was made only in the clear concentration areas of the precipitation diagram (Fig. 2, areas I-III) for systems with constant concentration of NaDBS, c_{NaDBS} = $2.5 \cdot 10^{-7}$ and $2.0 \cdot 10^{-6}$ mol dm^{-3}, and variable c_{DACl}; as well as for systems with constant concentration of DACl, c_{DACl} = $2.5 \cdot 10^{-7}$ and $2.0 \cdot 10^{-6}$ mol dm^{-3}, and variable c_{NaDBS} (Table 2). Besides this, examination was made for clear regions along equimolar line of the precipitation diagram, having in mind that above concentration of $1.5 \cdot 10^{-5}$ mol dm^{-3} phase separation occurs and vesicles are formed. The determined *cmc* of the equimolar DACl-NaDBS aqueous mixture is $3.25 \cdot 10^{-6}$ mol dm^{-3} (Fig. 6). The maximum surface excess, Γ_{max}, and the minimum area occupied per molecule, A_{min}, adsorbed at the air/solution interface in individual surfactant solutions and in their mixtures of different compositions, including equimolar one at the $cmc_{DACl\text{-}NaDBS}$, are presented in Table 2. The data concerning NaDBS, from *cmc*, A_{min} to γ, from this work are in excellent agreement with literature values [9, 24, 25, 30]. The addition of an oppositely charged surfactant decreases γ more drastically, indicating stronger interaction between surfactants, noticed even at the lowest examined concentrations. At the same time this addition increases total concentration of surfactant at the air solution interface, and simultaneously reduces the area occupied by one surfactant molecule. According to calculated *P* values, spherical to ellipsoidal micelles form in the region with DACl in excess; and curved bilayer structures, vesicles, or planar bilayer structures-lamellae, in the mixtures with NaDBS in excess. Furthermore, there is a tendency for the formation of bilayer structures in equivalent mixtures, as calculated (Table 2) and seen in Figs. 2 and 4. Results for mixed micelles formed in systems with constant DACl and varied NaDBS concentrations, point to almost no change in the surface charge density with the increased DACl concentration. On the other hand, higher NaDBS concentration in mixtures with varied DACl content induces higher increase of the apparent degree of chloride ion dissociation from the micelle/solution interface, α_{Cl}. This is attributed to either diversity in micellar size and/or shape, or differences in interactions between headgroups and counterions, whose main reason is distinct ion polarizability [13]. Somewhat lower apparent degree of counterion dissociation for equimolar mixtures of DACl and NaDBS arises from closer packing of the headgroups and higher surface charge density in the micelle/solution interface. Table 3 shows calculated concentrations for the same value of surface tension γ = 40 mN m^{-1} (Fig. 6), and these are c_{DACl} = $6.09 \cdot 10^{-3}$ mol dm^{-3}, c_{NaDBS} = $1.59 \cdot 10^{-3}$ mol dm^{-3}, $c_{DACl+NaDBS}$ = $2.09 \cdot 10^{-6}$ mol dm^{-3}. The composition of the mixed

monolayer and mixed micelle, the related surface activity coefficients, f_{DACl} and f_{NaDBS}, and the monolayer and mixed micelle interaction parameters, β_{mon} and β_{mic}, for systems containing equimolar mixtures (Table 3) were calculated using the Regular Solution Theory and Rubingh treatment for nonideal mixing [20]. A relatively high negative value of β indicates strong attractive interactions between oppositely charged surfactants, in both mixed monolayer and mixed micelles. Additionally, molar ratios of DACl in monolayers and in mixed micelles are similar.

Fig. 6

Table 3

Standard free energy change of adsorption, ΔG^o_{ads}, and free energy change of micellization, ΔG^o_{mic}, for DACl-NaDBS systems with corresponding parameters of individual NaDBS and DACl solutions were calculated and compared (Table 4). The results for DACl are in accordance with previously established data [31]. Increase of concentration of one surfactant in mixtures favors both adsorption and micellization. Both ΔG^o_{mic} and ΔG^o_{ads} are negative; adsorption is more spontaneous and thermodynamically favored with respect to micellization. The adsorption of mixed surfactants, especially for equimolar mixture, is more favorable than that of pure surfactants, as it was previously noticed [32]. Different structural and environmental factors may affect interactions during micellization and, consequently the values of *cmc* and free energy changes of micellization, ΔG^o_{mic}. Having in mind the hydrophobic part of ionic surfactants, several examples given in the literature consider most frequently the hydrophobic tail influence, neglecting other structural factors, such as pyridinium [33], or imidazole ring [33]. Generally, the phenyl ring in a *p*-benzenesulfonate is equivalent to about three and one-half methylene groups [21]. For determining the effective length of the branched hydrophobic group, the carbon atoms on the branches appear to have about one-half the effect of carbon atoms on a straight chain [34], and in the case of 4-(1-pentylheptyl) benzenesulfonate this means 6 C-atoms. Also, we must take the one between an ionic and a polar group in the molecule that is equal to about one-half of a C-atom on the main chain, and one methylene unit which connects branch and a phenyl ring. Totally, the effective length of hydrophobic part of the 4-(1-pentylheptyl) benzenesulfonate of amounts 11 methylene groups. Taking into account calculated ΔG^o_{mic} (Table 4), 12 methylene groups for individual DACl, 11 methylene groups for individual NaDBS solutions, and 23 methylene groups for DACl-NaDBS mixtures, it can be concluded that for mixtures with equimolar

proportion calculated values involved in the transfer of a methylene unit of the hydrophobic chain from an aqueous environment to the micelle are close to literature values [21], whereas for individual components and mixtures with either constant DACl and variable NaDBS concentration or *vice versa*, these values are slightly lower.

Table 4

Thermal and mesomorphic properties

As previously mentioned, the elemental analysis revealed the formation of the catanionic molecular complex DA-DBS, $C_{12}H_{25}NH_3^{\cdot}C_{18}H_{29}O_3S$, *i.e.* $C_{30}H_{57}NO_3S$, consisting of oppositely charged surfactants in equimolar proportions, according to relation:

$$C_{12}H_{25}NH_3^+ + Cl^- + Na^+ + C_{18}H_{29}SO_3^- \rightarrow \mathbf{C_{30}H_{57}NO_3S} + Na^+ + Cl^-.$$

The process took place at high concentration of surfactants (Fig. 2, point **D**), where vesicles breakage occurred and the less soluble catanionic salt, DA-DBS (Fig. 3d) precipitated from water.

Besides lyotropic properties, catanionic compounds frequently form thermotropic phases [14, 15]. Alkylammonium benzenesulfonates, naphthalenesulfonates and related salts form smectic (Sm) A mesophases [35, 36]. Most known symmetrical and asymmetrical catanionic compounds based on alkylammonium are bilayered structures [3, 4], but also some of them, such as alkylammonium-AOT complexes, form hexagonal columnar phases [16]. Characteristic textures of powdered DA-DBS formed upon heating and cooling are shown in Fig. 7, indicating lamellar organizations. Fig. 8 and Table 5 present transition temperatures and the resulting thermodynamic parameters. The DA-DBS sample was heated from RT to 400 K and cooled back to RT. WAXS measurement at 298 K (Fig. 9) confirmed the existence of layer-like arrangement *i.e.* crystal Sm structure. Sharp peaks with short range fluctuations, recognizable interlamellar distance and the ratio of spacings between allowed reciprocal lattice Bragg reflections (1:2:3: …) at 298 K are displayed on Fig. 9 and Table 6. There is also a weak diffuse peak in the diffraction pattern, with the vicinity of 4.5 Å, characteristic for flexible and disordered hydrocarbon chains. The established basic lamellar thickness d_{001} is 22.65 Å at 298 K. The most probable ion-pair amphiphilic cluster at room temperature consists of ionic groups formed in ordered layers with dodecyl chains packed into somewhat

disordered layers to accommodate. Taking into account the maximum lengths of hydrophobic parts (l_1= 1.668 nm and l_2 = 1.332 nm) and effective ionic radii of ammonium and sulfonate groups ($å_1$ = 0.25 nm and $å_2$ = 0.40 nm) [37], the calculated length of extended DA-DBS molecule is $d_c = l_1 + l_2 + 2å_1 + 2å_2$ = 4.300 nm. Therefore, the dodecyl chains must be tilted to the layer plane at β_t = 58 ^{o}, as established earlier for alkylammonium alkylsulfates [3].

Fig. 7

Fig. 8

Table 5

The DA-DBS complex melts at 346 K and transforms from solid to liquid crystalline state, till isotropisation at 368 K. All transitions are endothermic in the heating cycle and exothermic and with temperature hysteresis in the corresponding cooling cycle. The liquid crystalline state is seen through pseudoisotropic texture with Maltese crosses and oily streaks (Fig, 7 b–d), characteristic for lamellar Sm phases. Similar results of SmA phase formation were observed for dodecylbenzenesulfonic acid [38] on heating. The low enthalpy changes of the liquid crystalline-isotropic phase transitions and *vice versa* point also to structural changes involving transformations of Sm mesophase. The temperature interval of mesomorphic state stretches within the range of 22 K during heating and within 15 K on cooling. Crystallization of liquid crystal started at 344 K with nucleation in a spot (Fig. 7e) and proceeded in a radial fashion, leading to focal conic fan textures characteristic for SmC ordering (Fig. 7f). The transitions of solid DA-DBS are classified as enantiotropic.

Fig. 9

Table 6

Conclusions

The study of DACl and NaDBS aqueous mixtures reports interfacial, micellar and thermodynamic properties. The *cmc* values are lowered in the mixed state. Large negative free energy change favors the adsorption process. General phase behavior of aqueous mixtures confirms lyotropic properties of examined system. The calculated critical packing parameter in the regions of equivalent mixtures and those with excess of NaDBS, indicates formation of curved (vesicles) or planar (lamellae) bilayer structures, while in mixtures with DACl in excess spherical to ellipsoidal micelles are favored. Increment of surfactant concentration causes vesicle diameter growth and polydispersity, spontaneous transition of micelles via vesicles to lamellar, onion and extremely large elongated tubular phases.

Thermal properties of anhydrous catanionic ion-pairing compound DA-DBS were studied by optical microscopy, differential scanning calorimetry and X-ray diffraction. The title compound is classified as solid crystalline with rich thermotropic behavior and as enantiotropic liquid crystal. The most probable ion-pair amphiphilic cluster of crystal smectic phase, at room temperature, consists of ionic groups formed in ordered layers with dodecyl chains packed into somewhat disordered layers, tilted to the layer plane.

Acknowledgments

The authors are pleased to acknowledge support of this work by the Ministry of the Science, Education, and Sport of the Republic of Croatia (Project No 098-0982915-2949). We are grateful to Mr. sc. Vesna Vrdoljak in realization of partial precipitation diagram, to Dr. sc. D. Matković-Čalogović, Faculty of Science, University of Zagreb, for the X-ray diffraction measurements of the samples, and to Nikola Paić for his help with manuscript preparation.

References

1. Jokela P, Joensson B, Khan A (1987) Phase equilibria of catanionic surfactant-water systems. J Phys Chem 91:3291–3298.

2. Marques E, Khan A, da Graca Miguel M, Lindman B (1993) Self-assembly in mixtures of a cationic and an anionic surfactant: the sodium dodecyl sulfate-didodecyldimethylammonium bromide-water system. J Phys Chem 97:4729–4736.

3. Tomašić V, Popović S, Filipović-Vinceković N (1999) Solid State Transitions of Asymmetric Catanionic Surfactants. J Colloid Interface Sci 215:280–289.

4. Filipović-Vinceković N, Pucić I, Popović S, Tomašić V, Težak Đ (1997) Solid-Phase Transitions of Catanionic Surfactants. J Colloid Interface Sci 188:396–403.

5. Kaler EW, Murthy AK, Rodriguez BE, Zasadzinski JA (1989) Spontaneous vesicle formation in aqueous mixtures of single-tailed surfactants. Science 245:1371–1374.

6. Kaler EW, Herrington KL, Murthy AK, Zasadzinski JAN (1992) Phase behavior and structures of mixtures of anionic and cationic surfactants. J Phys Chem 96:6698–6707.

7. Rosen MJ, Li F, Morrall SW, Versteeg DJ (2001) The Relationship between the Interfacial Properties of Surfactants and Their Toxicity to Aquatic Organisms. Environ Sci Technol 35:954–959.

8. Mungray AK, Kumar P (2009) Fate of linear alkylbenzene sulfonates in the environment: A review. Int Biodeter Biodegr 63:981–987.

9. Ma J-G, Boyd BJ, Drummond CJ (2006) Positional isomers of linear sodium dodecyl benzene sulfonate: solubility, self-assembly, and air/water interfacial activity. Langmuir 22:8646–8654.

10. Das S, Bhirud RG, Nayyar N, et al. (1992) Chemical shift changes on micellization of linear alkyl benzenesulfonate and oleate. J Phys Chem 96:7454–7457.

11. Van Os NM, Daane GJ, Bolsman TAB. (1987) The effect of chemical structure upon the thermodynamics of micellization of model alkylarenesulphonates: I. Sodium p-(x-Decyl)benzenesulphonate isomers. J Colloid Interface Sci 115:402–409.

12. Chakraborty S, Chakraborty A, Ali M, Saha SK (2010) Surface and Bulk Properties of Dodecylbenzenesulphonate in Aqueous Medium: Role of the Nature of Counterions. J Disp Sci Technol 31:209–215.

13. TomaŠić V, Štefanić Z, Filipović-Vinceković N (1999) Adsorption, association and precipitation in hexadecyltrimethylammonium bromide/sodium dodecyl sulfate mixtures. Colloid Polymer Sci 277:153–163.

14. Filipović-Vinceković N, TomaŠić V (2000) Solid-State Transitions of Surfactant Crystals. In: Garti N (ed) Thermal Behavior of Dispersed Systems. M. Dekker Inc., New York-Basel, pp 451–476.

15. Filipović-Vinceković N, TomaŠić V (2002) Solid-Phase Transitions of Ionic Surfactants. In: Hubbard A (ed) Encyclopedia of Surface and Colloid Science. M. Dekker Inc., Santa Barbara, pp 4718–4736

16. Ungar G, TomaŠić V, Xie F, Zeng X (2009) Structure of Liquid Crystalline Aerosol-OT and Its Alkylammonium Salts. Langmuir 25:11067–11072.

17. Dai Q, Laskowski JS (1991) The Krafft point of dodecylammonium chloride: pH effect. Langmuir 7:1361–1364.

18. Compostizo A, Martín C, Rubio RG, Crespo Colin A (1996) Temperature dependence of the density of an ionic micellar system near the critical point. Chem Phys 212:301–310.

19. Zana R (1980) Ionization of cationic micelles: Effect of the detergent structure. J Colloid Interface Sci 78:330–337.

20. Rubingh DN (1979) Mixed Micelle Solutions. In: Mittal K. (ed) Solution Chemistry of Surfactants. Plenum Press, New York, NY, USA, pp 337–354.

21. Rosen MJ (1989) Surfactants and interfacial phenomena. Wiley & Sons Inc., New York, NY, USA.

22. Israelachvili JN, Mitchell DJ, Ninham BW (1976) Theory of self-assembly of hydrocarbon amphiphiles into micelles and bilayers. J Chem Soc, Faraday Trans 2 72:1525.

23. Rosen MJ, Aronson S (1981) Standard free energies of adsorption of surfactants at the aqueous solution/air interface from surface tension data in the vicinity of the critical micelle concentration. Colloids Surf 3:201–208.

24. Šegota S, Horbaschek K, Težak Đ (2001) Structure of sodium 4-(1-pentylheptyl)benzenesulphonate aggregates in water solutions by small angle X-ray scattering. Colloids Surf A 193:109–116.

25. Težak D, Hertel G, Hoffmann H (1991) Phase behaviour of n-alkyl- and bi-alkylbenzenesulphonates. Nematic lyotropics from double chain surfactants. Liq Cryst 10:15–27.

26. Binana-Limbelé W, van Os N., Rupert LA., Zana R (1991) Micelle aggregation numbers in aqueous solutions of sodium alkylbenzenesulfonates. J Colloid Interface Sci 141:157–167.

27. Težak Đ, Jalšenjak N, Punčec S, Martinis M (1997) Fractal approach to the liquid crystal formation of alkylbenzenesulphonates in solutions. Colloids Surf A 128:273–275.

28. Olsson U, Wennerström H (2002) On the Ripening of Vesicle Dispersions. J Phys Chem B 106:5135–5138.

29. Karukstis KK, McCormack SA, McQueen TM, Goto KF (2004) Fluorescence delineation of the surfactant microstructures in the CTAB-sOS-H2O catanionic system. Langmuir 20:64–72.

30. Binana-Limbelé W, van Os N., Rupert LA., Zana R (1991) Micelle aggregation numbers in aqueous solutions of sodium alkylbenzenesulfonates. J Colloid Interface Sci 141:157–167.

31. Filipovic-Vincekovic N, Bujan M, Juranovic I Adsorption and association in binary mixtures of cationic surfactants. J Disp Sci Technol 20:1737–1758.

32. Moulik SP, Haque ME, Jana PK, Das AR (1996) Micellar Properties of Cationic Surfactants in Pure and Mixed States. J Phys Chem 100:701–708.

33. Mehrian T, de Keizer A, Korteweg AJ, Lyklema J (1993) Thermodynamics of micellization of n-alkylpyridinium chlorides. Colloids Surf A 71:255–267.

34. Gotte E, Schwuger MI (1969) Uberlegungen und Experimente zum Mechanismus des Waschprozesses mit priméiren Alkyl sulfaten. Tenside 6:131—135.

35. Ito M, Matsunaga Y, Matsuzaki H, Shimojima S The thermotropic liquid-crystalline behavior of alkylammonium benzenesulfonates and related salts. Bull Chem Soc Jpn 62:3919–3922.

36. Matsunaga Y, Tsujimura T (1991) The Thermotropic Liquid-Crystalline Behavior of Alkylammonium Naphthalenesulfonates. Mol Cryst Liquid Cryst 200:103–108.

37. Lange NA, Dean JA (1979) Lange's Handbook of chemistry. McGraw-Hill.

38. Saupe A, Maier W (1961) Methods for Determining the Degree of Order in Nematic Liquid Crystal Layer. Z Naturforsch 16 a:816.

Author Biographies

Tea Mihelj, dipl.ing. is a research assistant and PhD student (Physical Chemistry) in the Laboratory for Synthesis and Self-Organization Processes of Organic Molecules, Division of Physical Chemistry, at the Ruđer Bošković Institute. Zagreb: University of Zagreb. She is an active member of Croatian Society of Chemical Engineers, Technical committee for surfactants (Croatian Standards Institute) and Croatian Microscopy Society.

Dr. Vlasta Tomašić is a senior research associate at the Ruđer Bošković Institute, Division of Physical Chemistry, Laboratory for Synthesis and Self-Organization Processes of Organic Molecules. Her education activities and mentorships are maintained at J. J. Strossmayer University of Osijek and at Faculty of Science, University of Zagreb; and applied activities at Technical committee for surfactants, Croatian Standards Institute.

Their current research interests include issues about lyotropic and thermotropic liquid-crystalline mesophases; physicochemical properties of catanionic and biosurfactants; their solid phase transitions; and adsorption, association and precipitation in aqueous surfactants mixtures.

Table captions

Table 1 Weight percentage distribution of examined NaDBS positional isomers and different alkyl chain length homologues (no decyl homologues found).

Table 2 Critical micellization concentration *cmc*, maximum surface excess, Γ_{max}, minimum surface area per surfactant molecule, A_{min}, critical packing parameter, *P*, and apparent degree of counterion dissociation from the micelle/solution interface, α, for aqueous solutions of individual cationic DACl and anionic NaDBS surfactant; mixtures with constant NaDBS and varying DACl concentration, mixtures with constant DACl and varying NaDBS concentration; and for equimolar mixtures, at 303 K.

Table 3 Molar ratio of DACl, x_{DACl}, related values of activity coefficients f_{DACl} and f_{NaDBS} for mixed monolayer and mixed micelle, and related interaction parameters β_{mon} and β_{mic} for equimolar aqueous mixtures of DACl and NaDBS.

Table 4 Calculated standard free energy change of adsorption, ΔG^{o}_{ads}, and standard free energy change of micellization, ΔG^{o}_{mic} at 303 K, in the aqueous solution of pure DACl or NaDBS, and in the aqueous DACl-NaDBS mixtures.

Table 5 Transition temperatures *T*/K, enthalpy changes ΔH/kJ mol^{-1}, and entropy changes ΔS/J mol^{-1} K^{-1} of the examined DA-DBS.

Table 6 Interplanar spacings, *d*, Miller indices, *hkl*, and relative intensities, I_{rel}, for pure DA-DBS at 298 K.

Figure captions

Fig. 1 LC-ESI-MS/MS extracted ion chromatograms at *m/z* values chosen for determination of alkyl benzenesulfonate isomers.

Fig. 2 Precipitation diagram of the DACl and NaDBS aqueous mixtures obtained after one day of aging at 303 K. The solid line corresponds to clear (I–III)-turbid (IV, V) solution boundary with vesicular dispersion (solid circles). The bold line is the border of the turbid (IV)-precipitation (V) area and dotted line is the equimolar line. Short dotted lines with open circles refer to changes of the *cmc* with one of the surfactant in excess and small addition of oppositely charged surfactant, obtained by conductivity measurements. Concentration points **A**-**C** were additionally examined, and **D** represents the equivalent concentration point at which the solid catanionic compound is precipitated and isolated.

Fig. 3 Microscopy images of DACl and NaDBS aqueous mixtures at 303 K, at the stoichiometric bulk composition, after 24 hours of aging, observed using phase contrast. $c_{NaDBS} = c_{DACl}$ $6 \cdot 10^{-4}$ mol dm^{-3} (a), $8 \cdot 10^{-4}$ mol dm^{-3} (b, c), and $2 \cdot 10^{-3}$ mol dm^{-3} (d). The bar corresponds to 50 μm.

Fig. 4 Microscopy images of DACl and NaDBS aqueous mixtures at 303 K, with DACl in excess (a, b) marked as point **A** in precipitation diagram, and with NaDBS in excess (c, d) marked as **B**, taken 24 hours after preparation; under cross-polarizers (a, c) or using phase contrast (b, d). The concentrations are c_{NaDBS}/mol dm^{-3} = $1 \cdot 10^{-3}$ and c_{DACl}/mol dm^{-3} = $6 \cdot 10^{-3}$ (**A**), and c_{NaDBS}/mol dm^{-3} = $6 \cdot 10^{-3}$ and c_{DACl}/mol dm^{-3} = $6 \cdot 10^{-4}$ (**B**). The bar corresponds to 100 μm (a, c) and 50 μm (b, d).

Fig. 5 Size of vesicles prepared in the equimolar area of precipitation diagram, noted with **C** and observed within one week. Concentration of both components was $c_{NaDBS} = c_{DACl} = 1 \cdot 10^{-4}$ mol dm^{-3}. A population of small vesicles (open circles) was noticed after 2 minutes of

preparation. Parallel with their growth, a population of larger ones (solid circles) was formed, after *cca.* 3 days (4500 min) of aging.

Fig. 6 Surface tension, γ, as a function of individual surfactant concentrations NaDBS (open circle) and DACl (open triangle), and of equimolar mixtures of DACl and NaDBS (solid triangle), at 303 K. Concentrations of solutions that show the same value of γ = 40 mN m^{-1} are noted as C_1 for DACl, C_2 for NaDBS and $C_{1\text{-}2}$ for DACl-NaDBS mixture.

Fig. 7 Cross-polarized microscopy images of characteristic textures of catanionic compound DA-DBS at different temperatures, *T*/K, formed upon heating at 298 (a), 352 (b), 364 (c); and upon cooling at 355 (d); 344 (e**)**, and 298 (f). The bar corresponds to 500 μm (a), 100 μm (b), and 50 μm (c–f).

Fig. 8 Representative thermogram of DA-DBS. Solid line represents endothermic transitions in the heating, and dash line the exothermic transitions in the cooling cycle.

Fig. 9 Diffractograms of examined catanionic DA-DBS compound taken at 298 K.

Scheme 1 Geometric structures of cationic, anionic surfactant, and catanionic ion complex in aqueous solution. Cationic surfactant conforms the cone, and anionic double-tailed surfactant conforms the truncated cone. The catanionic complex, dodecylammonium-4-(1-pentylheptyl) benzenesulfonate forms truncated cone, *i.e.* cuplike structure, approaching the shape of cylinder.

Table 1 Weight percentage distribution of examined NaDBS positional isomers and different alkyl chain length homologues (no decyl homologues found).

Isomers	Undecyl	Dodecyl	Tridecyl
C_2– C_3	–	–	–
C_4	–	0.12	0.13
C_5	0.17	0.16	–
C_6	1.03	98.13	0.26

Table 2 Critical micellization concentration *cmc*, maximum surface excess, Γ_{max}, minimum surface area per surfactant molecule, A_{min}, critical packing parameter, *P*, and apparent degree of counterion dissociation from the micelle/solution interface, α, for aqueous solutions of individual cationic DACl and anionic NaDBS surfactant; mixtures with constant NaDBS and varying DACl concentration, mixtures with constant DACl and varying NaDBS concentration; and for equimolar mixtures, at 303 K.

	System	γ				κ	
		cmc /mol dm^{-3}	$\Gamma_{max} \cdot 10^6$ /mol m^{-2}	A_{min} /nm^2	***P***	***cmc*** /mol dm^{-3}	α
	DACl	$1.48 \cdot 10^{-2}$	2.73	0.61	0.34	$1.51 \cdot 10^{-2}$	0.29
	NaDBS	$3.10 \cdot 10^{-3}$	2.41	0.69	0.36	$3.15 \cdot 10^{-3}$	0.76
Mixtures	$c_{NaDBS} = 2.5 \cdot 10^{-7}$	$1.25 \cdot 10^{-2}$	3.11	0.53	0.39	$1.25 \cdot 10^{-2}$	0.39
	$c_{NaDBS} = 2.0 \cdot 10^{-6}$	$7.37 \cdot 10^{-3}$	4.05	0.41	0.50	$7.00 \cdot 10^{-3}$	0.80
	$c_{DACl} = 2.5 \cdot 10^{-7}$	$6.67 \cdot 10^{-4}$	4.88	0.34	0.60	$6.00 \cdot 10^{-4}$	0.79
	$c_{DACl} = 2.0 \cdot 10^{-6}$	$5.00 \cdot 10^{-4}$	5.19	0.32	0.64	$5.54 \cdot 10^{-4}$	0.80
	$c_{DACl} = c_{NaDBS}$	$3.25 \cdot 10^{-6}$	5.93	0.28	0.73	$3.00 \cdot 10^{-6}$	0.28

Table 3 Molar ratio of DACl, x_{DACl}, related values of activity coefficients f_{DACl} and f_{NaDBS} for mixed monolayer and mixed micelle, and related interaction parameters β_{mon} and β_{mic} for equimolar aqueous mixtures of DACl and NaDBS.

Mixed monolayer	$x_{DACl} = 0.48$ $f_{DACl} = 3.586 \cdot 10^{-4}$ $f_{NaDBS} = 1.260 \cdot 10^{-3}$	$\beta_{mon} = -29.17$
Mixed micelle	$x_{DACl} = 0.49$ $f_{DACl} = 4.083 \cdot 10^{-4}$ $f_{NaDBS} = 9.951 \cdot 10^{-4}$	$\beta_{mic} = -29.41$

Table 4 Calculated standard free energy change of adsorption, ΔG^{o}_{ads}, and standard free energy change of micellization, ΔG^{o}_{mic} at 303 K, in the aqueous solution of pure DACl or NaDBS, and in the aqueous DACl-NaDBS mixtures.

	System	$-\Delta G^{o}_{ads}$/kJ mol^{-1}	$-\Delta G^{o}_{mic}$/kJ mol^{-1}
	DACl	34.20	18.40
	NaDBS	32.30	17.90
Mixtures	$c_{NaDBS} = 2.5 \cdot 10^{-7}$	29.55	27.34
	$c_{NaDBS} = 2.0 \cdot 10^{-6}$	33.93	28.50
	$c_{DACl} = 2.5 \cdot 10^{-7}$	39.48	33.45
	$c_{DACl} = 2.0 \cdot 10^{-6}$	39.52	34.47
	$c_{DACl} = c_{NaDBS}$	60.43	52.21

Table 5 Transition temperatures T/K, enthalpy changes ΔH/kJ mol^{-1}, and entropy changes ΔS/J mol^{-1} K^{-1} of the examined DA-DBS.

Heating			**Cooling**		
T/K	ΔH/ kJ mol^{-1}	ΔS/ J mol^{-1} K^{-1}	T/K	ΔH/ kJ mol^{-1}	ΔS/ J mol^{-1} K^{-1}
346	40.8	117.9	344	–37.7	–109.6
368	0.2	0.5	359	–0.2	–0.4

Table 6 Interplanar spacings, *d*, Miller indices, *hkl*, and relative intensities, I_{rel}, for pure DA-DBS at 298 K.

d **/Å**	***hkl***	$\boldsymbol{I_{rel}}$
22.6522	001	100
11.3251	002	20
7.5507	003	76
5.6863	004	37
4.5428	005	64
3.7754	006	31
3.2360	007	22
2.9665		7
2.8315	008	12
2.3599		17
2.2633	0,0,10	4
1.9663		>1

Fig. 1 LC-ESI-MS/MS extracted ion chromatograms at *m/z* values chosen for determination of alkyl benzenesulfonate isomers.

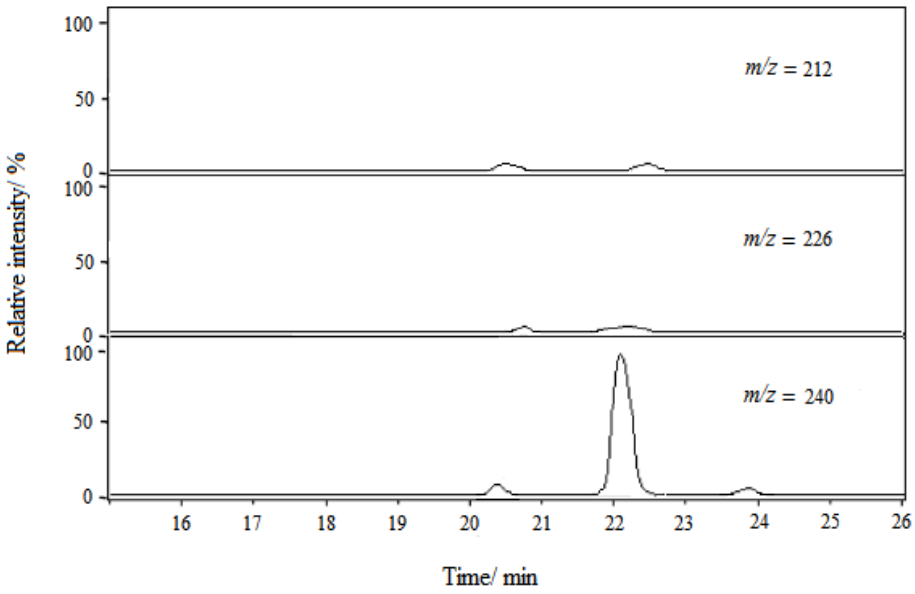

Fig. 2 Precipitation diagram of the DACl and NaDBS aqueous mixtures obtained after one day of aging at 303 K. The solid line corresponds to clear (I–III)-turbid (IV, V) solution boundary with vesicular dispersion (solid circles). The bold line is the border of the turbid (IV)-precipitation (V) area and dotted line is the equimolar line. Short dotted lines with open circles refer to changes of the *cmc* with one of the surfactant in excess and small addition of oppositely charged surfactant, obtained by conductivity measurements. Concentration points **A**-**C** were additionally examined, and **D** represents the equivalent concentration point at which the solid catanionic compound is precipitated and isolated.

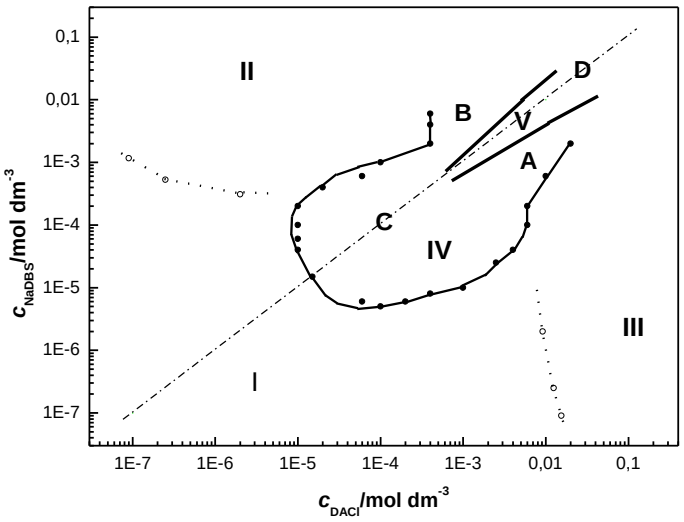

Fig. 3 Microscopy images of DACl and NaDBS aqueous mixtures at 303 K, at the stoichiometric bulk composition, after 24 hours of aging, observed using phase contrast. $c_{NaDBS} = c_{DACl}$ $6 \cdot 10^{-4}$ mol dm^{-3} (a), $8 \cdot 10^{-4}$ mol dm^{-3} (b, c), and $2 \cdot 10^{-3}$ mol dm^{-3} (d). The bar corresponds to 50 μm.

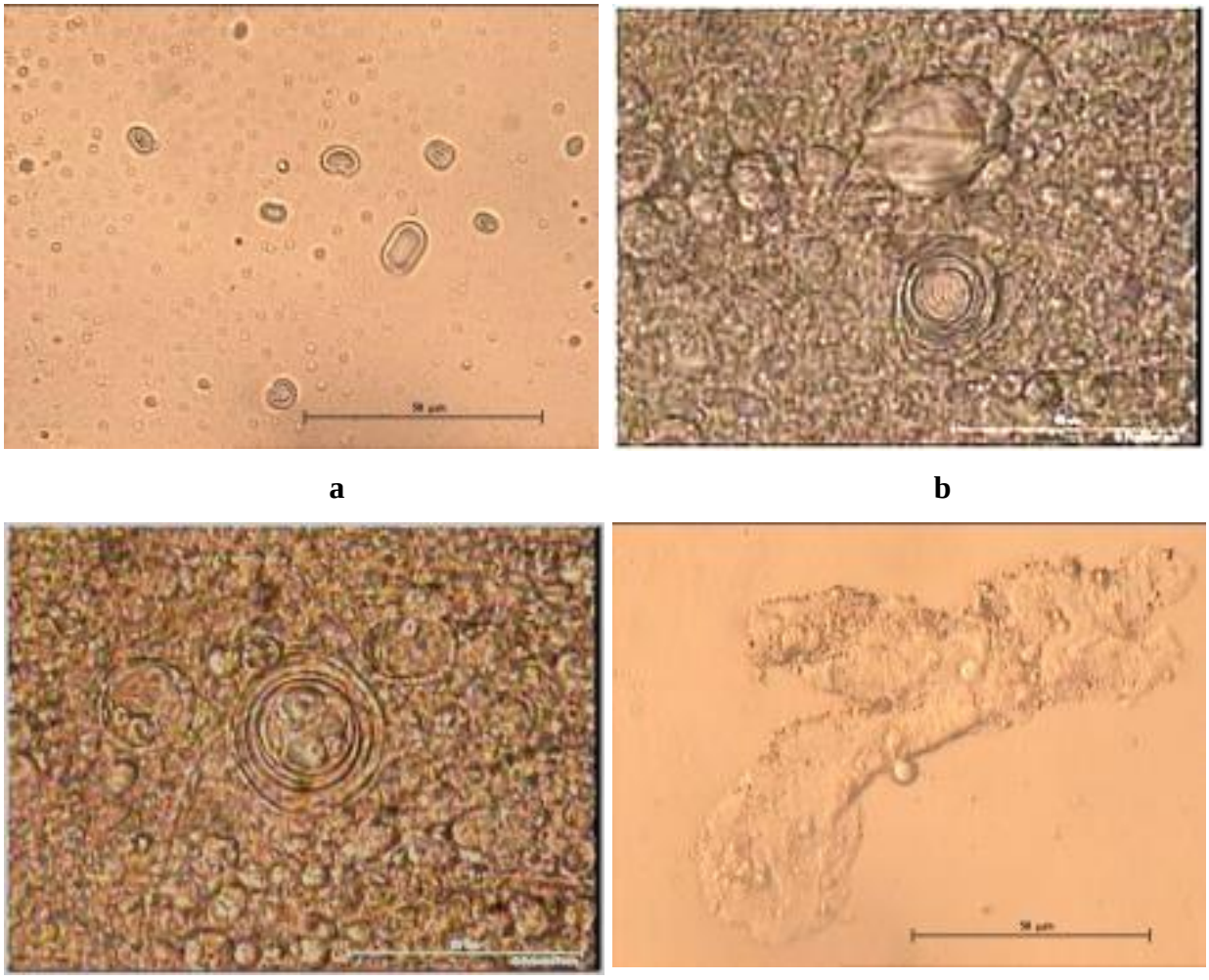

a **b**

c **d**

Fig. 4 Microscopy images of DACl and NaDBS aqueous mixtures at 303 K, with DACl in excess (a, b) marked as point **A** in precipitation diagram, and with NaDBS in excess (c, d) marked as **B**, taken 24 hours after preparation; under cross-polarizers (a, c) or using phase contrast (b, d). The concentrations are c_{NaDBS}/mol dm^{-3} = 1·10^{-3} and c_{DACl}/mol dm^{-3} = 6·10^{-3} (**A**), and c_{NaDBS}/mol dm^{-3} = 6·10^{-3} and c_{DACl}/mol dm^{-3} = 6·10^{-4} (**B**). The bar corresponds to 100 μm (a, c) and 50 μm (b, d).

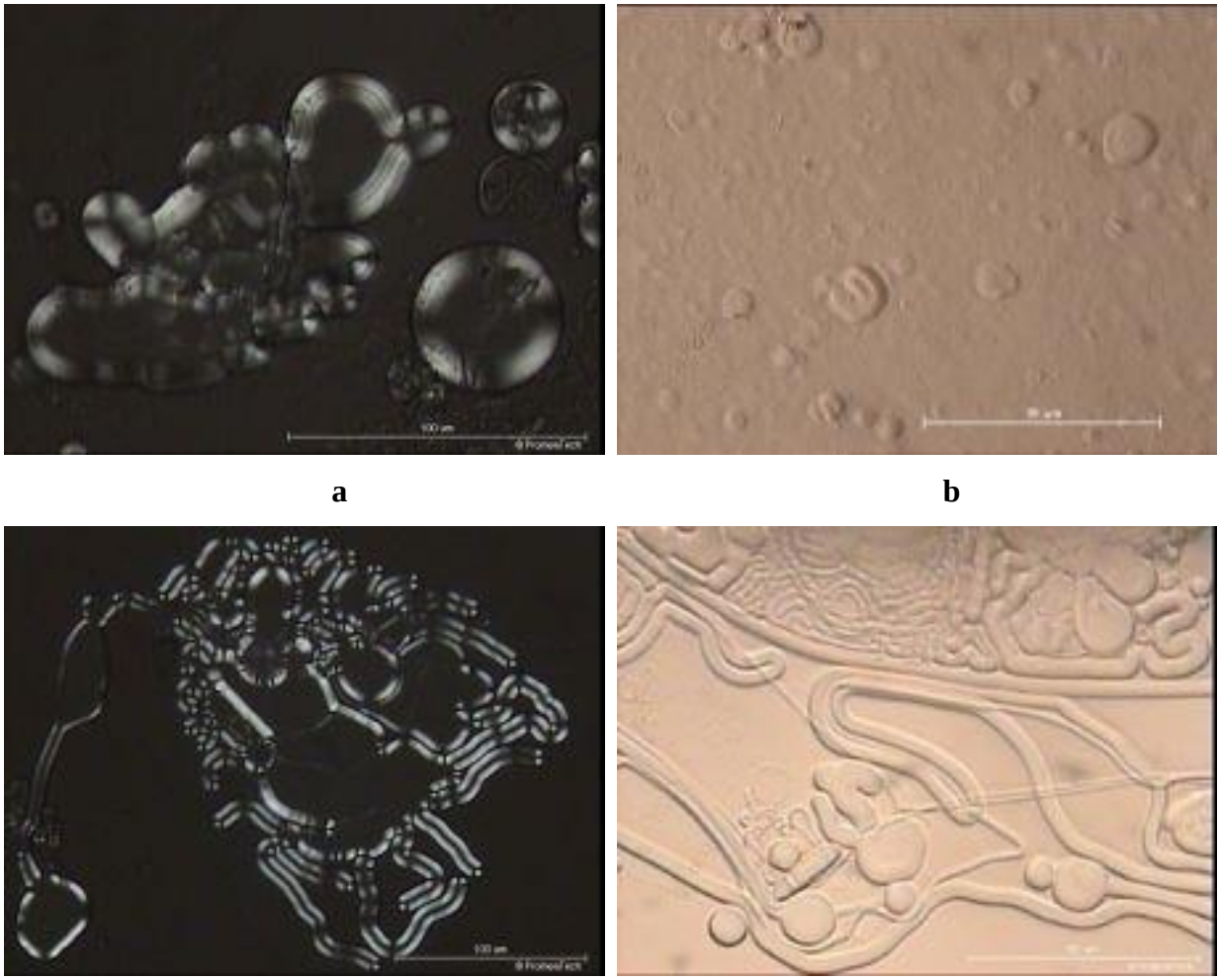

a **b**

c **d**

Fig. 5 Size of vesicles prepared in the equimolar area of precipitation diagram, noted with **C** and observed within one week. Concentration of both components was $c_{NaDBS} = c_{DACl} = 1 \cdot 10^{-4}$ mol dm^{-3}. A population of small vesicles (open circles) was noticed after 2 minutes of preparation. Parallel with their growth, a population of larger ones (solid circles) was formed, after *cca.* 3 days (4500 min) of aging.

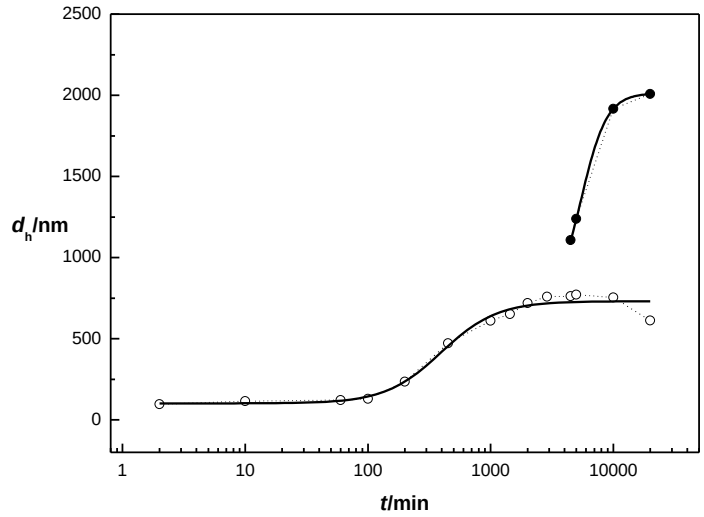

Fig. 6 Surface tension, γ, as a function of individual surfactant concentrations NaDBS (open circle) and DACl (open triangle), and of equimolar mixtures of DACl and NaDBS (solid triangle), at 303 K. Concentrations of solutions that show the same value of γ = 40 mN m^{-1} are noted as C_1 for DACl, C_2 for NaDBS and $C_{1\text{-}2}$ for DACl-NaDBS mixture.

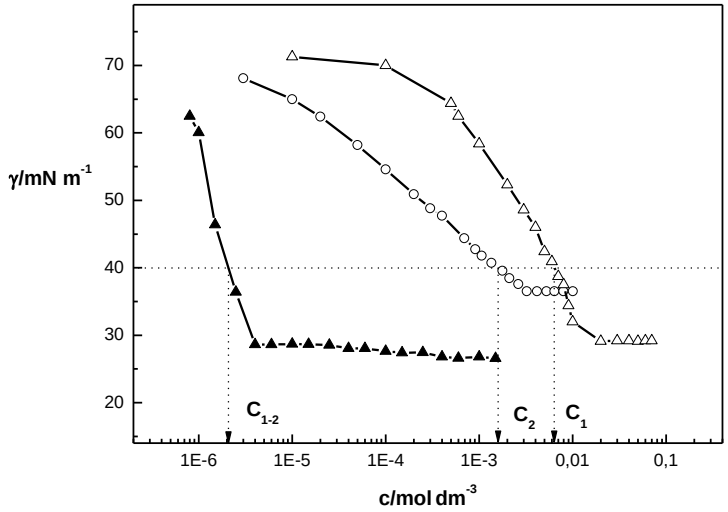

Fig. 7 Cross-polarized microscopy images of characteristic textures of catanionic compound DA-DBS at different temperatures, *T*/K, formed upon heating at 298 (a), 352 (b), 364 (c); and upon cooling at 355 (d); 344 (e**)**, and 298 (f). The bar corresponds to 500 μm (a), 100 μm (b), and 50 μm (c–f).

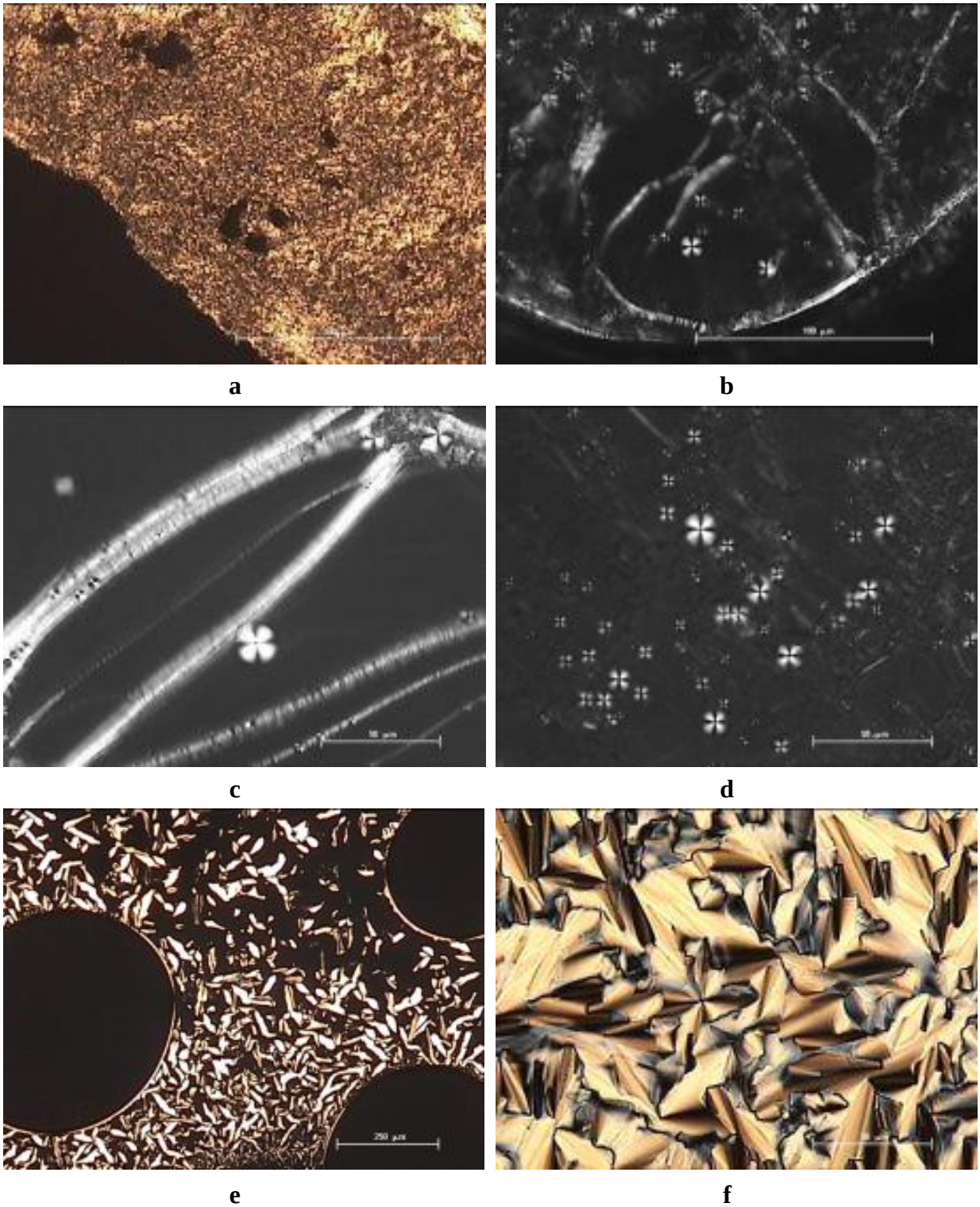

a **b**

c **d**

e **f**

Fig. 8 Representative thermogram of DA-DBS. Solid line represents endothermic transitions in the heating, and dash line the exothermic transitions in the cooling cycle.

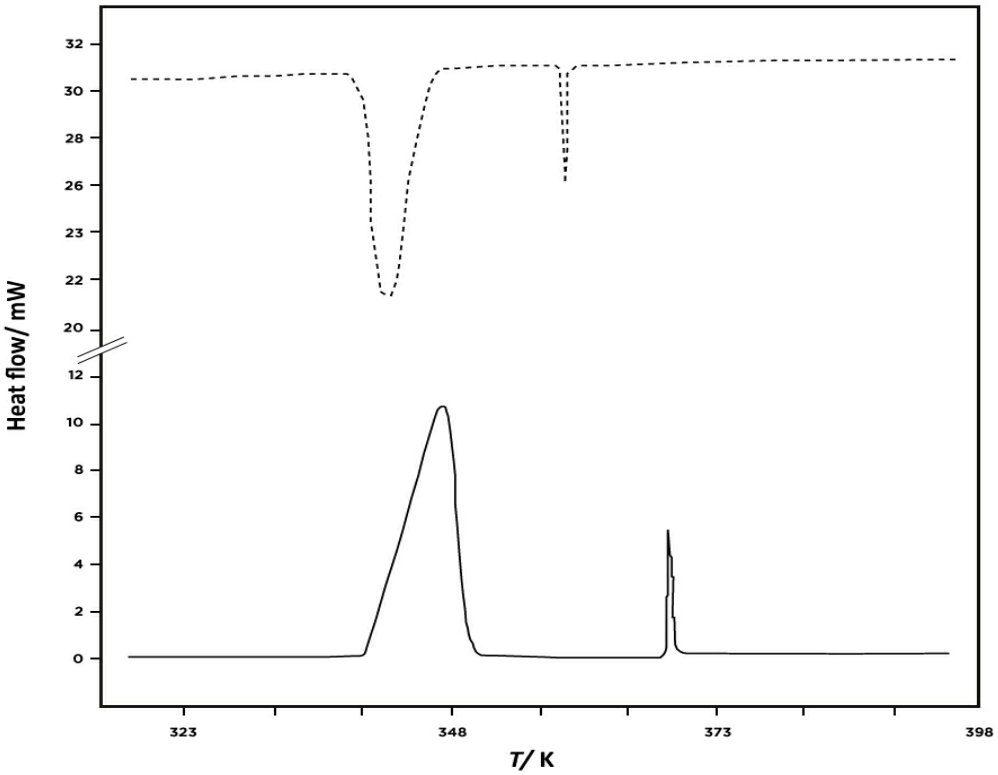

Fig. 9 Diffractograms of examined catanionic DA-DBS compound taken at 298 K.

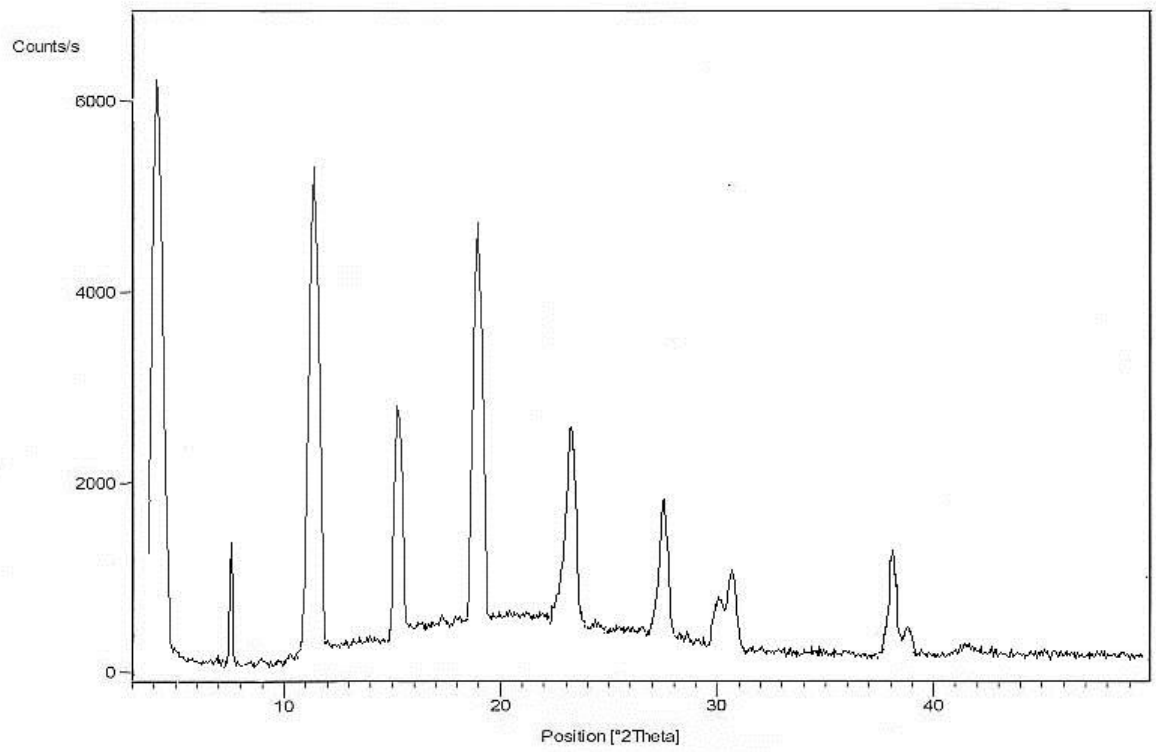

Scheme 1. Geometric structures of cationic, anionic surfactant, and catanionic ion complex in aqueous solution. Cationic surfactant conforms the cone, and anionic double-tailed surfactant conforms the truncated cone. The catanionic complex, dodecylammonium-4-(1-pentylheptyl) benzenesulfonate forms truncated cone, *i.e.* cuplike structure, approaching the shape of cylinder.